

Measuring sputter yields of ceramic materials

IEPC-2009-240

*Presented at the 31st International Electric Propulsion Conference,
University of Michigan • Ann Arbor, Michigan • USA
September 20 – 24, 2009*

Michael Tartz^{*}, Thomas Heyn[†], Carsten Bundesmann[‡] and Horst Neumann[§]
Leibniz-Institute of Surface Modification, Leipzig, 04318, Germany

This paper describes the sputter yield measurements on isolating materials. To avoid charging of the non-conducting target a neutralizer is employed. The target current is determined from reference measurements of a material with known sputter yield. Strong effects of the neutralizing electrons on the ion beam properties at the target were found. Therefore, a comprehensive characterization of the ion properties at the target has been performed. The sputter yield of quartz, alumina (Al₂O₃) and boron nitride (BN) under normal xenon ion incidence has been measured in the energy range 100 to 800 eV.

I. Introduction

When an energetic particle hits a material surface, it transfers energy and momentum to the material atoms; some of them can gain enough energy to leave the material. This process is called sputtering and is quantitatively described by the sputter yield as the average number of ejected particles per incident (energetic) particle. In electric propulsion, the detailed knowledge of the sputter yield is of high importance for lifetime estimations of the ion propulsion devices and all satellite components, which might be subject of ion impingement by the ion beam plume or ions from secondary processes. Also for terrestrial applications of plasmas and ion beams for various surface modification technologies the sputter yield is an important material and process parameter.

In gridded ion thrusters the lifetime is mainly limited by the erosion of the ion extraction grids due to impingement of charge-exchange ions¹. In a Hall thruster, the acceleration channel walls are suffering from strong erosion by ions from the discharge plasma². Other satellite components as solar arrays or optical elements can also be hit by primary beam or secondary ions, which might lead to a degradation of the component and affects its performance and, eventually, its lifetime.

Although there exists a large database of sputter yields, for many relevant material-target combinations one is faced with a lack of data. Particularly for compound materials like ceramics the supply of sputter data from literature is poor.

At IOM, sputter yield measurements of ion thruster grid materials like graphites³ and various metals⁴ have been performed. The pertinent sputter yields were found in a good agreement with results from other groups if available.

Recently, the interest has grown in the sputter behavior of isolating materials, which, however, is a much more complicated experimental task. The impingement of positively charged ions on the isolating surface leads to a charging of the surface, which affects the energy of the following arriving ions and has an influence on the ion beam transport to the target. In order to avoid the surface charging, the ion beam current has to be neutralized by adding a suitable amount of electrons to the beam. This implicates that it is no longer possible to measure the target current directly, which however is a required parameter.

The IOM sputter facility and procedures were adapted in order to measure sputter yields of an isolating material with a current-neutralized beam. A hot-cathode neutralizer was added to the ion source. The unknown target current is determined from a reference measurement of a material with a well-known sputter yield.

^{*} Senior scientist, Department of Ion Beam Technology, michael.tartz@iom-leipzig.de

[†] Master Student, University of Leipzig

[‡] Senior scientist, Department of Ion Beam Technology, carsten.bundesmann@iom-leipzig.de

[§] Senior scientist, Department of Ion Beam Technology, horst.neumann@iom-leipzig.de

At first, it was investigated how the neutralization influences the properties of the ion beam, which are essential for the sputter yield determination. The aim was to define the operation conditions and procedures in order to ensure long-time stable conditions and to define the target current. Initial sputter yield results are presented for quartz, alumina (Al_2O_3) and Boron Nitride (BN) under normal xenon ion incidence for energies between 100 and 800 eV.

II. Experimental setup

A. The sputter test facility

The sputter behavior is investigated in a dedicated UHV chamber at IOM (Figure 1), which is evacuated by a turbo pump (2000 l/s) to a background pressure of less than 10^{-8} mbar. As a result of the xenon gas flow through the ion beam source the process pressure increases up to $5 \cdot 10^{-5}$ mbar. The residual gas composition is permanently controlled by a quadrupole mass spectrometer yielding very low contents of water (many orders of magnitude lower than xenon), pure oxygen was not detected. This ensures that additional chemical etching on the sputter samples in presence of oxygen practically does not occur.

The samples are transferred into the vacuum chamber by a load-lock chamber and a pushing rod in order to keep the extraordinary vacuum in the measurement chamber.

The xenon ion beam is produced by an ISQ 40 DC Kaufman type ion source (Figure 2) as developed at IOM. The advantage of the Kaufman type ion source is the very well-defined ion energy and the very low energy spread compared to the previously used rf ion source (see section III.A). The initial beam diameter is 3 cm. A low divergence three-grid extraction system is used to apply a high ion current density up to 3 mA/cm^2 on the target. The source operates at ion energies up to 1200 eV, on the low-energy side practically down to a few electron volts. The source can be operated with almost all non-reactive gases, for the measurements presented here xenon gas is feed by a mass flow controller.

The sputter targets are placed in the beam centre at a distance of 13 cm from the grids. The targets can be tilted relative to the beam direction. For non-isolating targets the target current is directly measured and logged by a computer.

The measured target current has to be corrected by the amount of charge-exchange ions created between ion source and target, which contribute to the sputtering process but not to the current measurement⁵ by a factor e^{-nd} , with n being the neutral density, d the distance to the target and σ the charge-exchange cross section. The resulting correction factor was around 0.95.

Another correction to the target current had to be done for the occurrence of secondary electron emission during ion bombardment, which virtually increases the measured target current. The supply of experimental emission coefficients is poor particularly in the low energy region (i.e. < 1000 eV) under investigation here. The existing values suggest that the secondary electron emission is very low, therefore it was neglected.

The samples are weighed before and after sputtering employing a high-precision microbalance with a precision of $10 \mu\text{g}$. The sputter time had to be chosen large enough to obtain a reliable detectable mass difference (usually at least 1 mg). The sputter yield is estimated from the weight loss, the sputter time and the corrected target current.

The samples were prepared from the respective material (purity of at least 99.9%) as it was delivered. Before first measurement all samples were presputtered in order to avoid the influence of the surface roughness or the primary ion implantation and sticking on the sputter result. Most of the samples were sputtered consecutively many times.

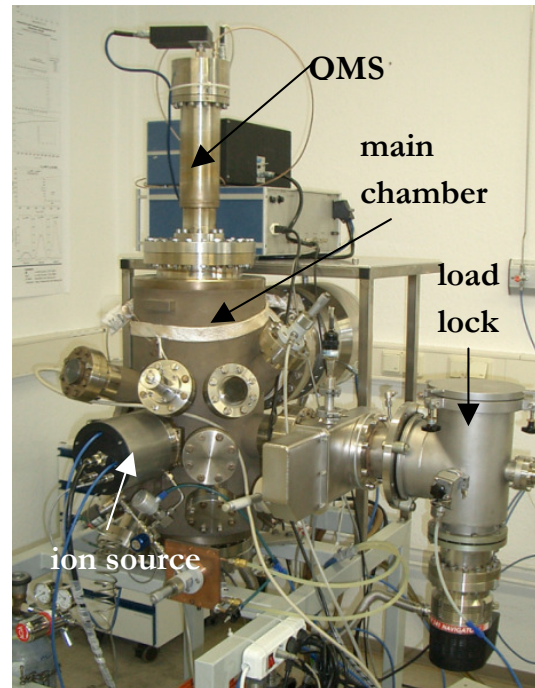


Figure 1: The IOM sputter test facility with load-lock, dc ion source and quadrupole mass spectrometer for residual gas analysis.

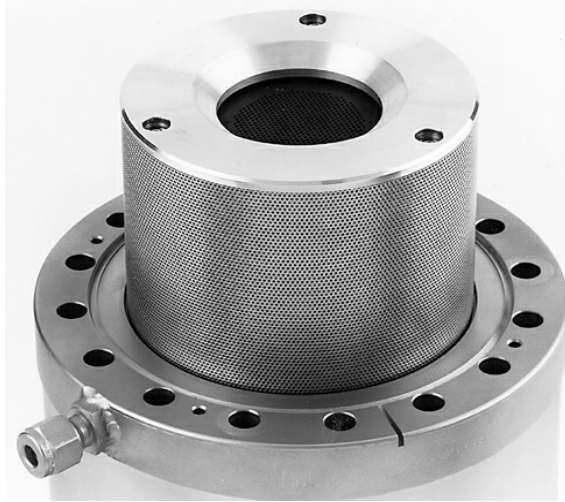


Figure 2: Kaufman type ion beam source ISQ40DC.

B. Modifications of the setup for isolating materials

The investigation of isolating materials requires the addition of electrons to the ion beam in order to avoid the charging of the target. A directly heated tungsten hot-filament neutralizer cathode is placed close to the ion beam. If the neutralizer filament is placed within the ion beam a very efficient coupling of the electrons to the beam is achieved. On the other hand, the lifetime of the filament is significantly reduced if it is directly hit by the ion beam. Because of the lifetime issue, in this study the filament was placed outside but closely enough to the ion beam enabling a coupling to the beam. This results in somewhat larger electron currents to obtain the same effect on the target as with an in-beam filament. The neutralizer can be set to an additional potential U_N . The emitted electron current is controlled by the applied heating current and the neutralizer potential U_N .

The target is now electrically isolated mounted, which enables measuring of the potential of the target U_{target} due to the charging. This value provides a reference for monitoring the experiment.

The sputter yield measurements were performed under conditions where the target is neutralized ($U_{target}=0V$). The target current is determined from a measurement with a material of well-known sputter yield. Here, silver was used, which has the advantage of a very high sputter yield and a low sputter threshold and therefore low sputter time even at low ion energies. Other materials were also tested for use as reference, no significant effect on the sputtering target current was found (see III.D).

C. Energy-selective Mass Spectrometry (ESMS)

ESMS allows to analyze the energy distribution of the ions and the beam composition regarding the ion mass and charge. A Hiden EQP-300 was used. Ions enter the device through a small aperture (see schematic setup in Figure 3). An ion optics transfers the ion beam to a electrostatic sector field energy analyzer (analyzing range up to 1000 eV, resolution 0.5 eV). Following this, a triple quadrupole mass filter separates the ions according to their mass-to-charge ratio up to a maximum of 300 amu, and finally a channeltron secondary electron multiplier with a dynamic range of 7 decades is used for ion counting. Further details of the device and function can be found elsewhere^{6,7}.

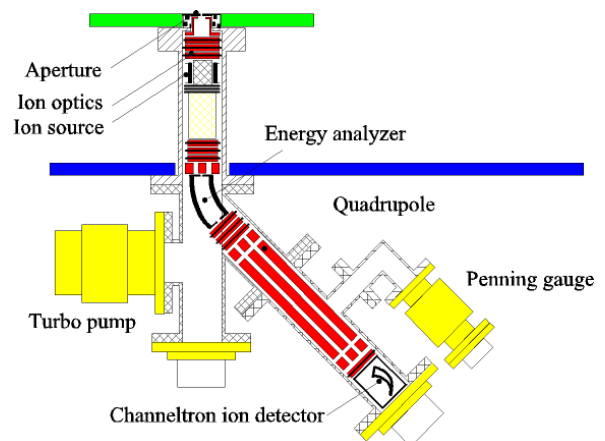


Figure 3: Setup of the Hiden EQP300.

III. Ion beam properties and neutralization effects

Precise knowledge of the amount and the properties of the sputtering particles is necessary for performing sputter measurements. While with conductive targets the determination of the ion energy and current is quite straightforward, the situation is more difficult in the case of an isolation target because of the added neutralizing electrons. Therefore, a comprehensive characterization of the ion beam has been performed in order to ensure the beam properties and verify the measurement principle.

A. The ion energy distribution

At first, the ion energy distribution of the used ion source ISQ40DC was investigated by ESMS. Figure 4 shows the energy spectra of ^{131}Xe isotope ions at various beam voltages. It can be seen, that the ion energy distribution is rather small (FWHM about 11 eV and below, increasing with ion energy) with a tail to lower energies of at least two orders of magnitude lower intensity. The main ion energy corresponds to the pre-set beam voltage also down to very low ion energies, which is characteristic for Kaufman type ion sources. Therefore, this source was selected for the sputter measurements.

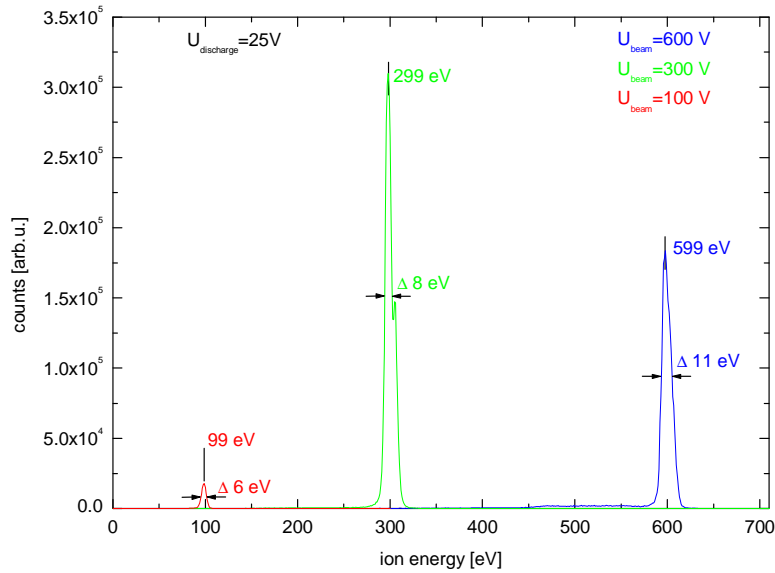


Figure 4: Energy distributions in the ion beam of the ISQ40DC ion source at various beam voltages.

The beam composition has been determined from the mass spectra, proving a very low content of double charged ions of below 1% thanks to the low discharge voltage of 25 V, which was used throughout this study. With increasing discharge voltage the content of double charged ions is growing.

B. Ion beam without neutralization

The ion beam was characterized without neutralization in order to define suitable operational parameters for sputter experiments. The beam current (I_{Beam}), the currents on the accelerator grid (I_{acc}), on the decelerator grid (I_{dec}) and the target current (I_{Target}) were taken in dependence on the accelerator voltage (U_{acc}) for ion energies of 800 eV and 100 eV.

In Figure 5 (left plot) it can be seen that for increasing accelerator voltage the beam current increases as expected. The currents on the accelerator and decelerator grids show a minimum. The target current has a maximum in the region of the minima of the currents on the grids. The behavior of the accelerator and decelerator currents shows the effect of direct impingement of beam ions on the grids for low accelerator voltage.

The right plot in Figure 5 shows the situation for a beam voltage of 100 V. The accelerator current for low accelerator voltage is high and decreases as the accelerator voltage increases. The decelerator current as well starts with a relatively high value and increases further with the accelerator voltage. The value of the target

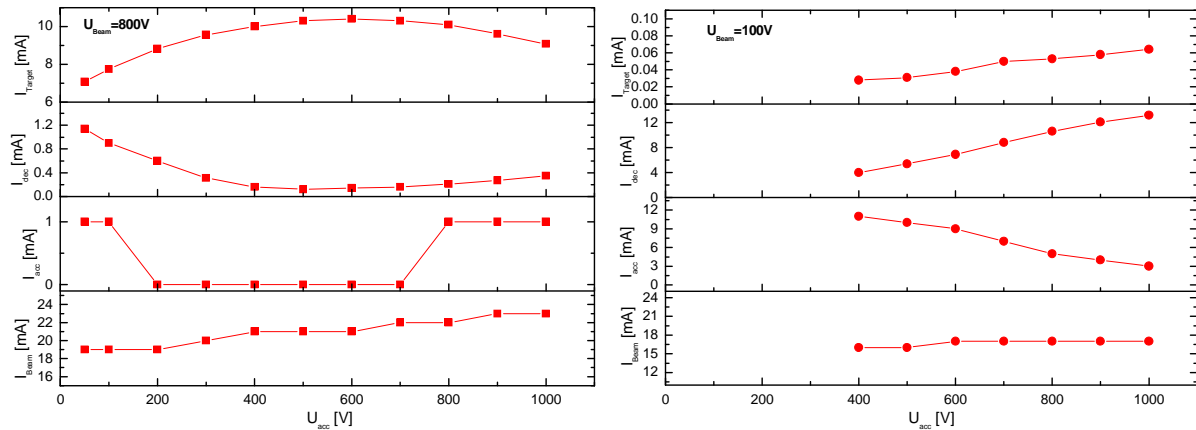


Figure 5: Ion beam and grid currents for a beam voltage of 800 V (left) and 100 V (right) at different plasma densities in dependence on U_{acc} . Please note that values of I_{beam} and I_{acc} were given by the power supply as integers. Target size is $2.5 \times 2.5 \text{ cm}^2$.

current is very low over the shown region (always $< 0.1 \text{ mA}$), almost all of the extracted ions arrive on one of the grids.

The reason for this striking unexpected behavior is believed to be that the compensation of the space charge induced by the ions is highly insufficient at $U_{beam}=100 \text{ V}$. It is assumed that the amount of electrons generated by ionization of beam ions and secondary electron emission at any wall at this low ion energy is not enough to compensate the space charge.

The IGUN⁸-simulations of a beamlet at a beam voltage of 100 V and an accelerator voltage of 1000 V with and without space charge compensation in Figure 6 illustrate that the ions are deflected at the space charge outside the source and that most of them hit the decelerator grid as the increased decelerator current in Figure 5 indicates as well. Hence, under these conditions, meaning the weak erosion of target material due to the low target current and the strong erosion of grid material, no sputter experiments are possible considering the required time to get a measurable change in target mass and the lifetime of the extraction grids.

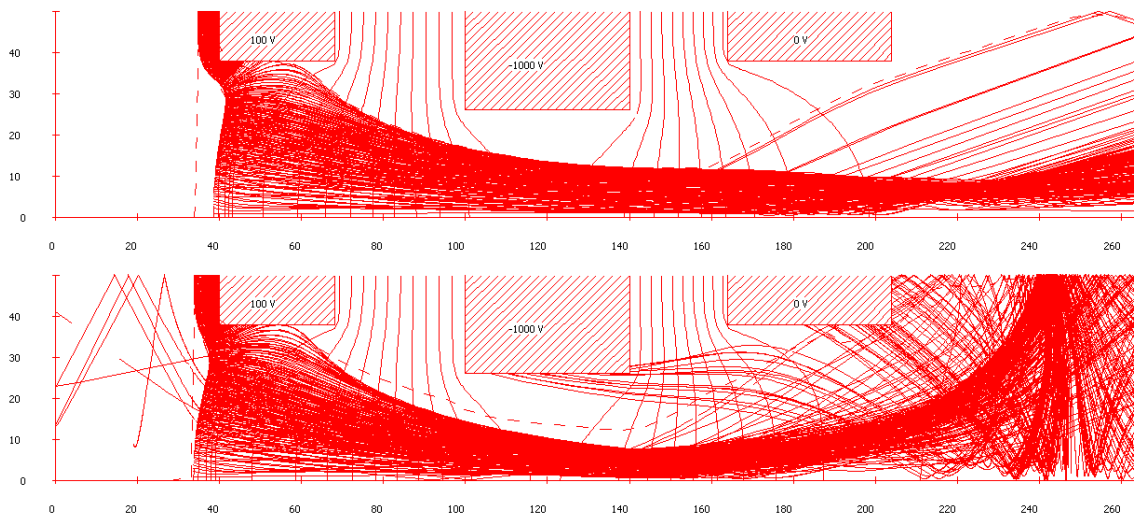


Figure 6: Simulation of beamlet at a beam voltage of 100 V with (top) and without space charge compensation (bottom).

This effect of insufficient neutralization can be found up to beam voltages of 300V (see Figure 7). Conspicuously, there is a sharp transition between the non-compensated and the compensated state. With increasing beam voltage the transition to the compensated state occurs at a higher value than the transition back to the non-compensated state with decreasing beam voltage (like a hysteresis). There is currently no satisfying explanation for this effect, further experiments are necessary.

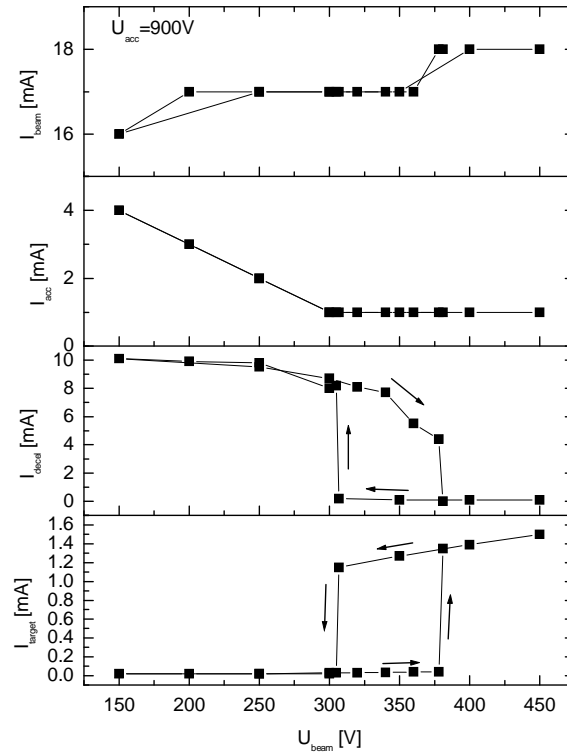


Figure 7: Ion beam and grid currents in dependence on the beam voltage U_{beam} . $U_{acc}=900V$

C. Ion beam with neutralization

In order to characterize the influence of the injected electrons on the beam properties the target current (I_{Target}) and the current on the decelerator grid (I_{dec}) were taken in dependence on the electron current $I_{electron}$. The target voltage (U_{Target}) was measured on the isolated target. The beam currents did not change significantly and are not shown here. The accelerator voltages were chosen according to Figure 5. An additional voltage U_N of -9 V was applied to the neutralizer.

In Figure 8 the influence of the injected electrons on the ion beam is shown for $U_{beam}=800$ V and 100V. It can be seen that the target voltage without additional electrons goes up to 530 V ($U_{beam}=800$ V) and 80 V ($U_{beam}=100$ V) corresponding to 65% and 80% of the beam voltage. The target voltage depends on the space charge potential, the incoming ion and electron currents and the secondary electron generation on the target.

At $U_{beam}=800$ V, the target current increases up to an electron current of 10 mA with growing electron current, the maximum is 3% higher than for the case with zero electron current. For a further increasing electron current

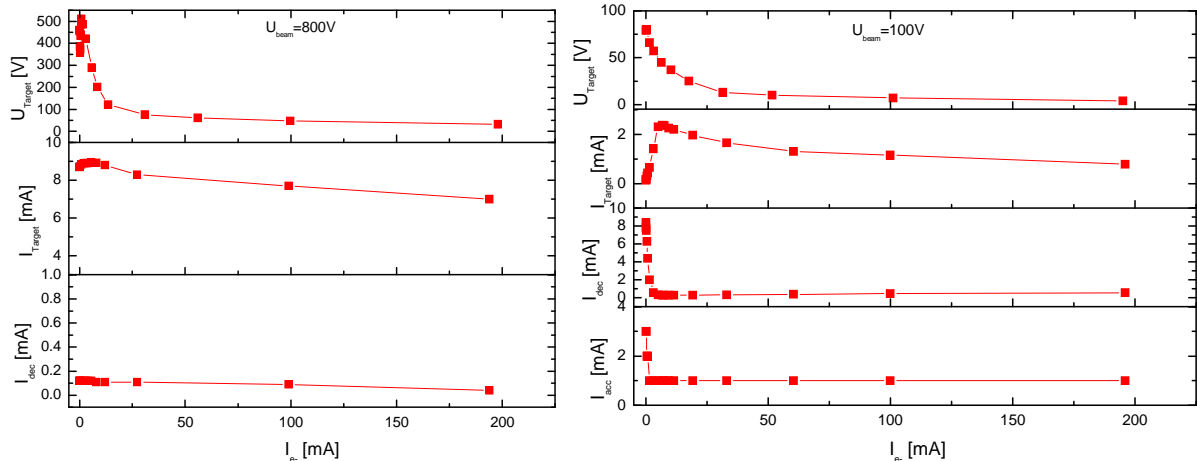


Figure 8: Influence of electrons on ion beam and target for a beam voltage of 800 V (left) and 100 V (right).

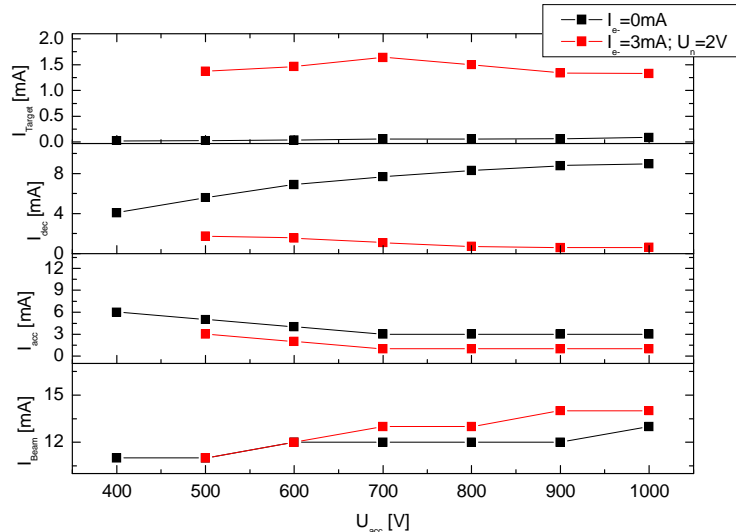


Figure 9: Comparison of ion beam properties with and without electron emission at $U_{beam}=100V$.

the target voltage and the target current decrease as more electrons reach the target. To obtain a neutralized target with this setup very high electron currents are needed. The decelerator current is only slightly influenced. At $U_{beam}=100V$, already a few electrons (<3 mA) have a strong effect on the ion beam. The currents on the accelerator and the decelerator grid are reduced to reasonable values. The target voltage starts at 80 V and decreases with increasing electron current. For $I_{electron} \approx 5$ mA the target current reaches its maximum which is 20 times the value with zero electron current.

The possible explanation for these strong effects is that the emitted electrons significantly enhance the space charge compensation. The few added electrons are able to initiate further ionization processes at the residual gas and secondary processes at surfaces, which results in an increased number of electrons for the space charge compensation. While without additional electrons most of the ions return towards the ion source, now the ion beam leaves the grids and moves through the chamber. Consequently, the ion beam behaves as it would be expected as is shown in Figure 9. The inset of direct impingement was found at $U_{acc}=800$ V, corresponding to $U_{extraction}=900$ V, which agrees well to the value for $U_{beam}=800$ V (see Figure 5).

In order to further characterize the ion beam profile on an isolating target, the footprint of the beam on SiO_2 -layers of known thickness on silicon wafers was investigated. The thickness of the SiO_2 -layers after sputtering was measured optically (see example in Figure 10). For a better comparability of the various conditions the erosion rate Δs in nm/min is determined and used.

It was found, that the position of the beam center is independent on the electron current with respect to the accuracy of the measurement (see Figure 11). The non rotational symmetric filament neutralizer has obviously no effect on the beam symmetry, no asymmetric beam profiles were found.

The erosion rate at the beam center (Δs_{max}) strongly increases for small amounts of injected electrons (see Figure 12). The growing maximal erosion rate agrees well with the strong increase of the target current and the reducing target charging (Figure 8, right plot). For further increasing electron current the maximum erosion rate reduces, also the total erosion of the eroded volume reduces. This can be traced back only to a reduced target current as it is demonstrated in the next section.

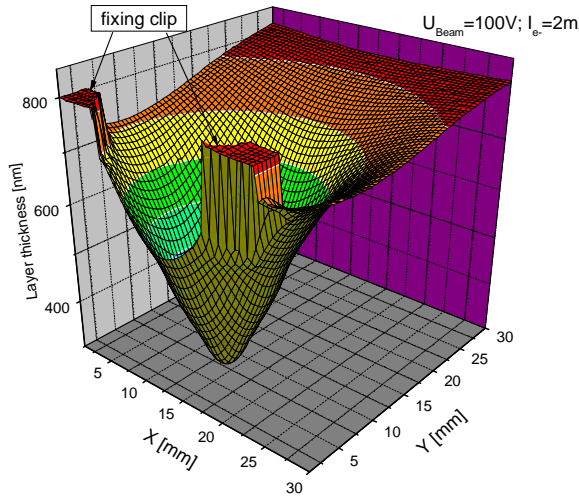


Figure 10: Measured thickness of SiO₂-layer after sputtering at a beam voltage of 100 V (initial value is 800 nm)

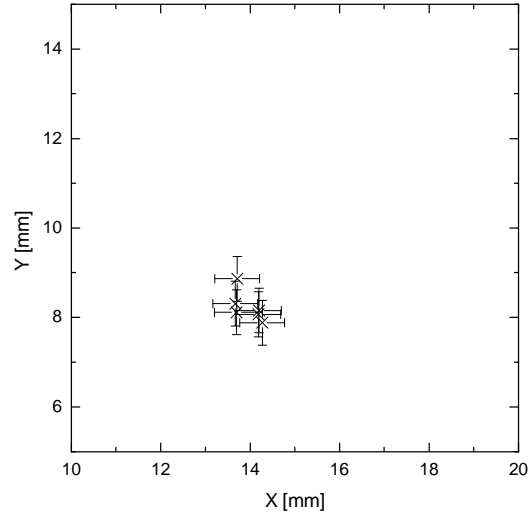


Figure 11: Center of ion beam for different electron currents (2, 5, 20, 100 and 195 mA)

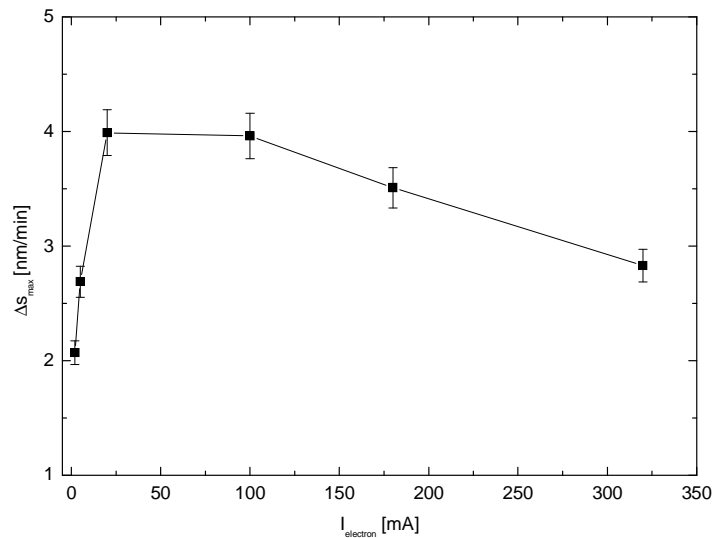


Figure 12: Erosion rate at beam center (maximum erosion rate) Δs_{\max} for SiO₂ sputtered at a beam voltage of 100 V.

D. Target current

The target current has been directly measured from a molybdenum and aluminum target in dependence on the neutralizer voltage U_N , i.e. the negative potential applied to the neutralizer cathode **. This potential is usually set negative in order to increase the amount of electrons emitted by the cathode according to the space-charge limited conditions. The electron current has been set to 4.5 mA. As shown in Figure 13, the target current drops when the neutralizer is set to a few volts negative and then increases with U_N (i.e. U_N gets more negative, see footnote). When exceeding about 40V, the target current differs for both materials. The secondary electron emission coefficient (SEEC) for electron impact is larger for molybdenum than for aluminum (clean) (see Figure 14) [9, 10], the coefficients apparently differ at energies above 50 eV. The larger SEEC of molybdenum virtually increases the target current more than with aluminum as can be seen in the figure.

** Please note that U_N gives the absolute value of the negative potential.

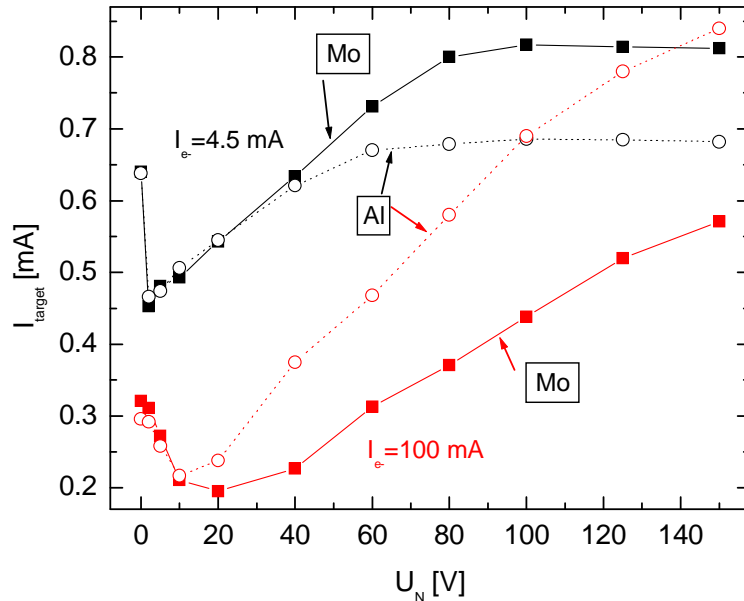


Figure 13: Directly measured target current at $U_{beam}=100$ V and electron currents of 4.5 mA (black curves) and 100 mA (red) for molybdenum (full symbols) and aluminum (open symbols) in dependence on the neutralizer voltage.

With the higher electron current of 100 mA the measured target currents are lower (compare to Figure 8), however, the measured current of the higher-SEEC material molybdenum is lower than that of aluminum. The reason for this contrary behavior is currently ambiguous.

The directly measured target currents are affected by the rather unknown content of electrons arriving at the target. The electrons could be suppressed by biasing the target which, however, may produce other effects on the ion beam.

In order to determine the content of ions (i.e. the sputtering particles), reference measurements were performed using a material with a well-known sputter yield. The effective sputtering current $I_{target,sput}$ is determined from the mass loss, the sputter time and the known sputter yield. This procedure is also used to determine the target current before any sputter measurement of isolating materials.

This approach largely avoids all participation of the electrons on the target current, but depends on the assumption that the sputtering particles have a well-known energy. The ion energy is affected by the target potential, which can be measured in case of a conducting target, but which can only be approximated in case of an isolating target material to be the same as that of the sample mounting parts. The ion energy distribution has been investigated (see section III.A) to correspond accurately to $e \cdot U_{beam}$ (grounded target).

It has been found that the sputtering target current strongly depends on the electron parameters. Figure 15 shows the target current $I_{target,sput}$ and target potential in dependence on the electron current for silver and tungsten targets (the target potential has been considered in the sputter yield for calculating the target current). Figure 16 gives the target current in dependence on the neutralizer potential U_N for a fixed electron current.

With growing electron current the $I_{target,sput}$ shows a maximum which is found at a target voltage of about 18 V. A further growing electron current reduces the sputtering target current. At $U_{beam}=500$ V, for a neutralized target an electron current of 300 mA is required, the sputtering target current is 20% lower than at the maximum. At 100 V, similar relations are found. The sputtering target current reduces with growing electron current.

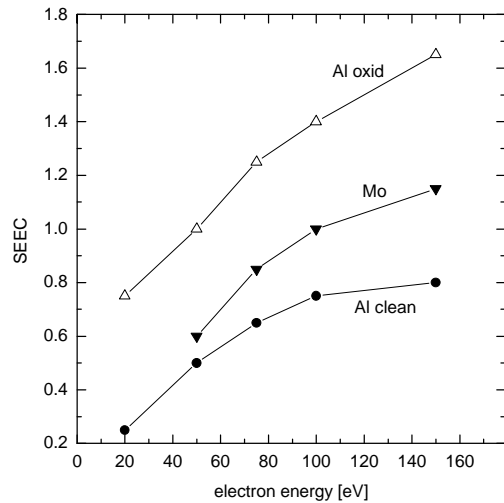


Figure 14: Secondary electron emission coefficients in dependence on electron energy. Data from [9, 10]

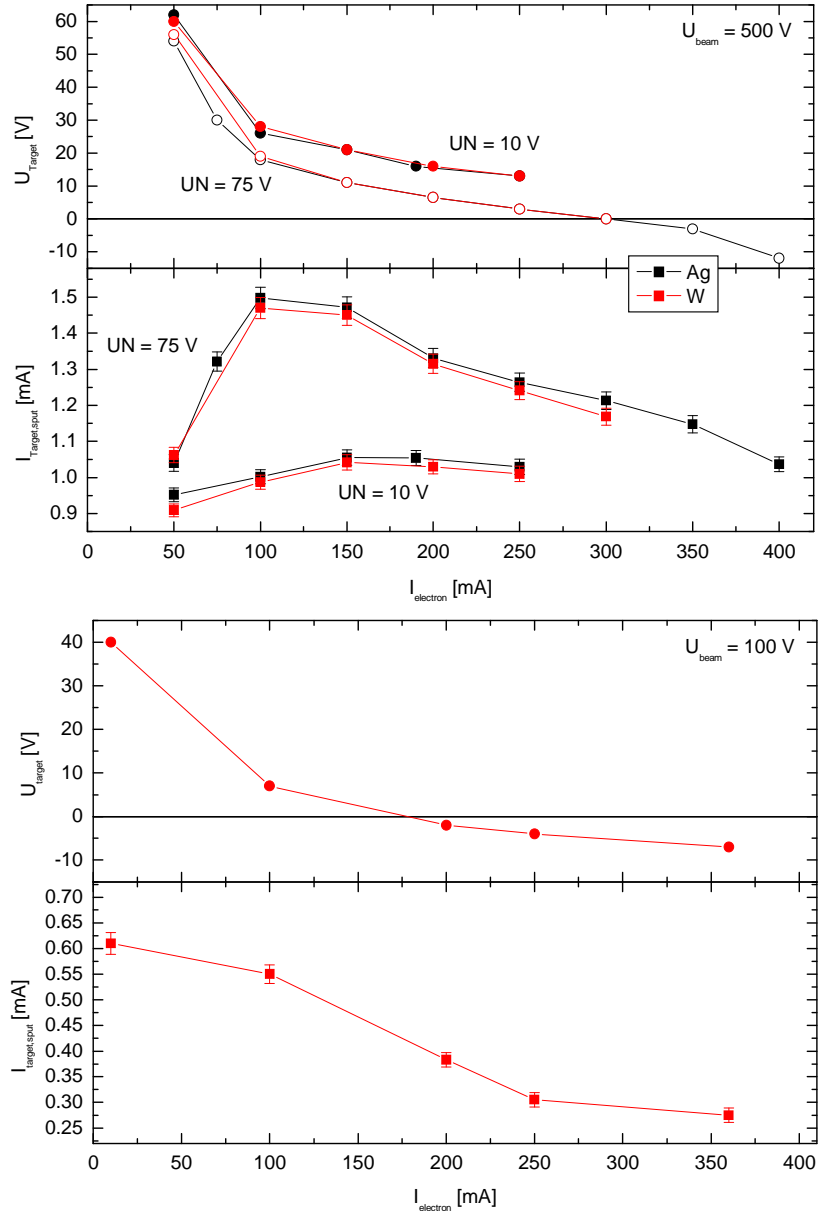


Figure 15: Effective sputtering target current $I_{Target,sput}$ and target potential U_{Target} in dependence on electron current. Top: $U_{beam}=500\text{V}$. Bottom: $U_{beam}=100\text{ V}$. Target potential considered for current determination.

Increasing neutralizer voltage U_N leads to a larger sputtering target current and a lower target charging (Figure 16).

No significant effect of the material on the effective sputtering target current was found as it was expected. The slightly lower currents found for tungsten compared to silver (about 2%) are traced back to a slight underestimation of the used tungsten sputter yield model (Bohdansky formula³) as compared to own measurements at tungsten.

Furthermore, a slight decrease of the sputter yield of BN at larger U_N was found (see Figure 17) which is traced back to the effect of the secondary electrons on the target charging and the space charge within the ion beam. For U_N up to 30 V no effect on the sputter yield can be seen.

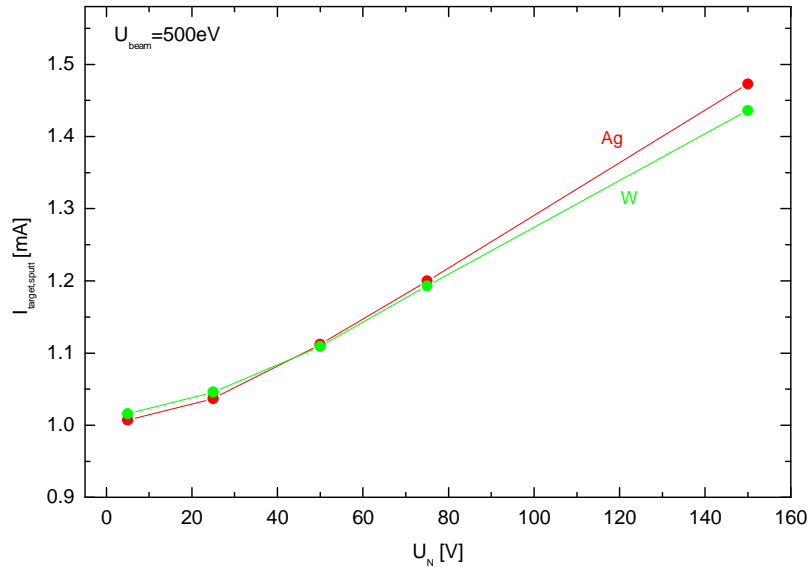


Figure 16: Effective sputtering target current in dependence on neutralizer voltage U_N . $U_{\text{beam}}=500$ V, $I_{\text{beam}}=18$ mA, I_{electron} set to have zero target voltage.

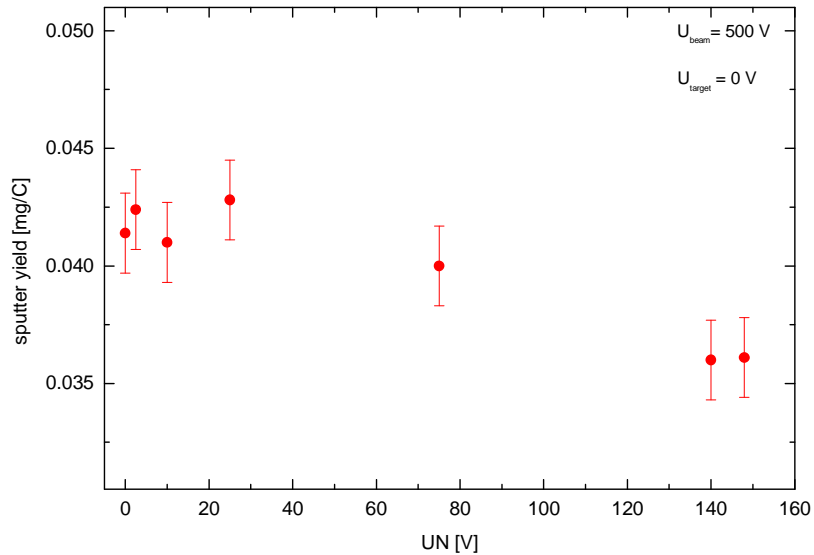


Figure 17: Sputter yield of BN measured at various neutralizer voltages U_N . Electron current set to $U_{\text{target}}=0$ V.

E. Conclusions for the sputter measurements

For reliable sputter measurements precise knowledge of the properties of the sputtering ions is necessary. Therefore, the effects of the neutralizing electrons on the ion beam and the target have been investigated thoroughly. Strong impacts of the electron conditions on the space charge, the target charging, the ion beam properties and, consequently, the properties of the sputtering particles were found.

The results of the beam characterization suggest to perform the sputter experiments at large neutralizer voltages and lower electron currents where the resulting target current is maximum. However, the target is not neutralized under such condition which falsifies the sputter yields because of the affected ion energy. Therefore, it was decided to perform the sputter yield measurements at lower neutralizer voltages (typically 25V were used) and at electron currents where the target potential measured at the reference target is equal or slightly below zero volt.

These results demonstrate the complex nature of the sputtering target current under neutralized beam conditions. In consequence, the target current has to be measured before each sputter experiment.

IV. Sputter yields of ceramics

The sputter yields of ceramic materials have been measured under normal xenon incidence at 100, 250, 350, 500 and 800 eV. The results are given in mm^3/C corresponding to the removed volume per Coulomb of incoming particles. For multicomponent materials as ceramics the usual sputter yield unit “atoms/ion” is not applicable because the single components may be sputtered differently (preferential sputtering). This leads to an equilibrium surface composition which may differ from the initial composition.

Our results are compared with available literature data if possible.

A. Sputter yields of quartz and Al_2O_3

Figure 18 shows the sputter yields of quartz and alumina under normal xenon ion incidence. Our quartz data is somewhat lower than the results of Yalin et. al.¹¹. A good agreement with simulated sputter yields of Tondou et. al.¹² is found. No other experimental data is found for alumina.

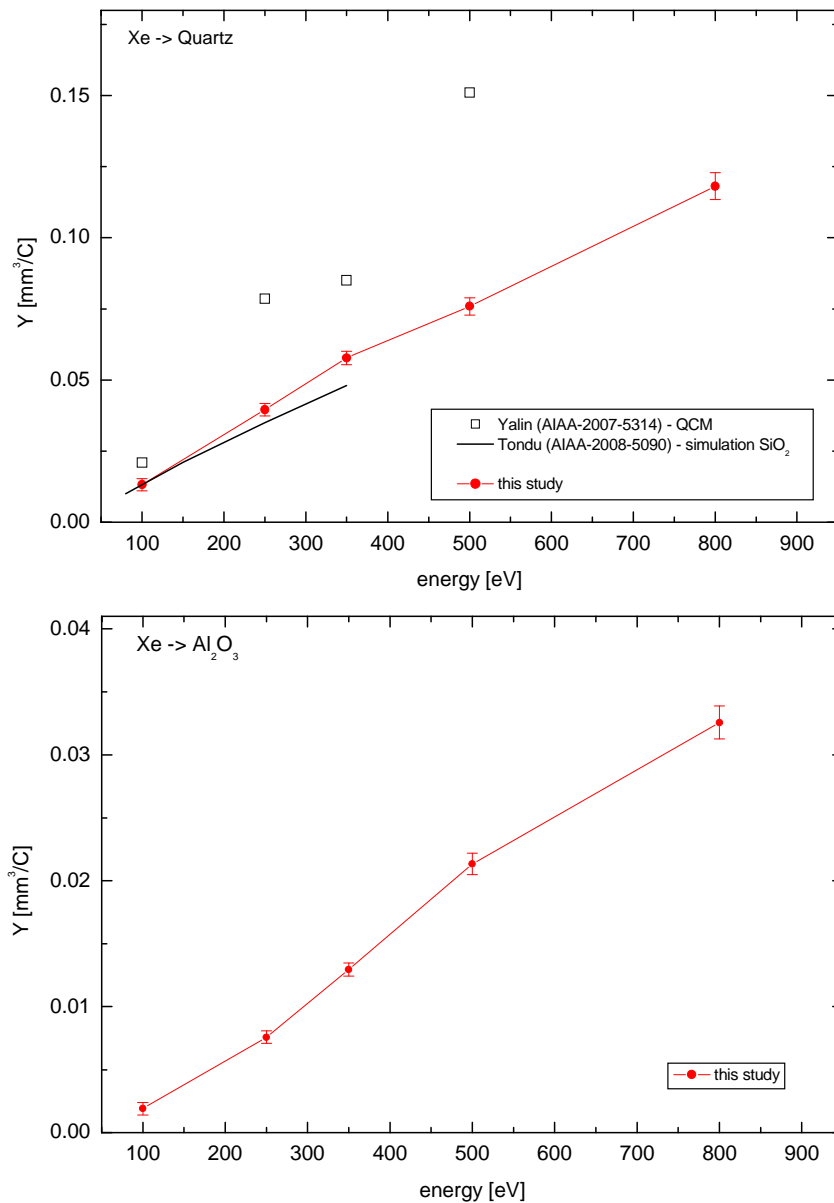


Figure 18: Sputter yields of quartz (top) and alumina (Al_2O_3) in dependence on xenon ion energy.

B. Sputter yield of BN

The sputter yields were measured using an isotropic pressed high-density BN with Calcium Borate binder (samples provided by Sindlhauser Materials).

As already reported by others¹³ BN shows significant moisture absorption. As shown in Figure 19 the mass of the BN sample increases after taking the sample out of the vacuum to normal atmosphere. After about 8 hours the steady-state is reached. Although this total mass increase is only less than 0.2% of the sample mass, it is in the order of the mass change by sputtering. In order to ensure reliable mass values all samples were weighed after at least 8 hours at normal atmosphere (practically done at the next day). The effect of varying humidity at different days on the mass was found to be within the weighing measuring error.

Figure 20 shows the BN sputter yields in comparison with other published data^{13 - 17}. Our yields are the lowest and are in agreement with the 2007 CSU weight loss data of HBC grade BN by Rubin et. al.¹³. Newer data from the same group by Topper et. al.¹⁷ show much higher sputter yields, the reason for this discrepancy is currently not clear and under investigation. The agreement with simulated data by Tondou et. al.¹² is very good.

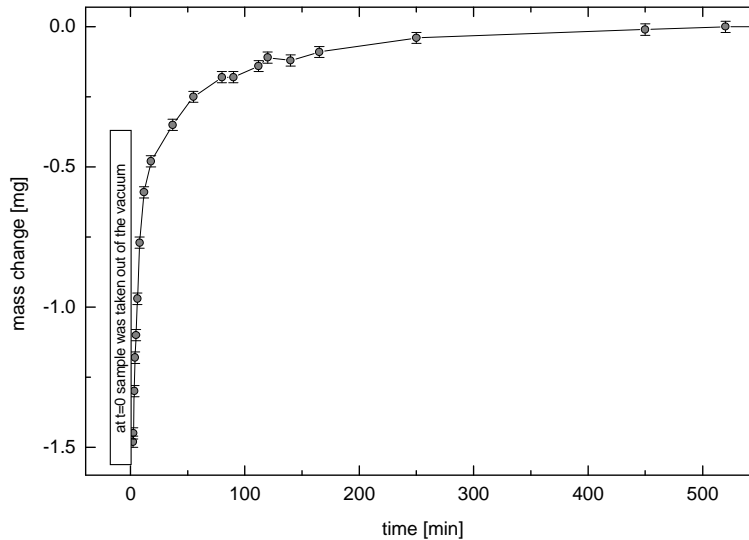


Figure 19: Moisture absorption of BN sample after 4h xenon bombardment (500 eV). Sample was taken out of the vacuum at t=0.

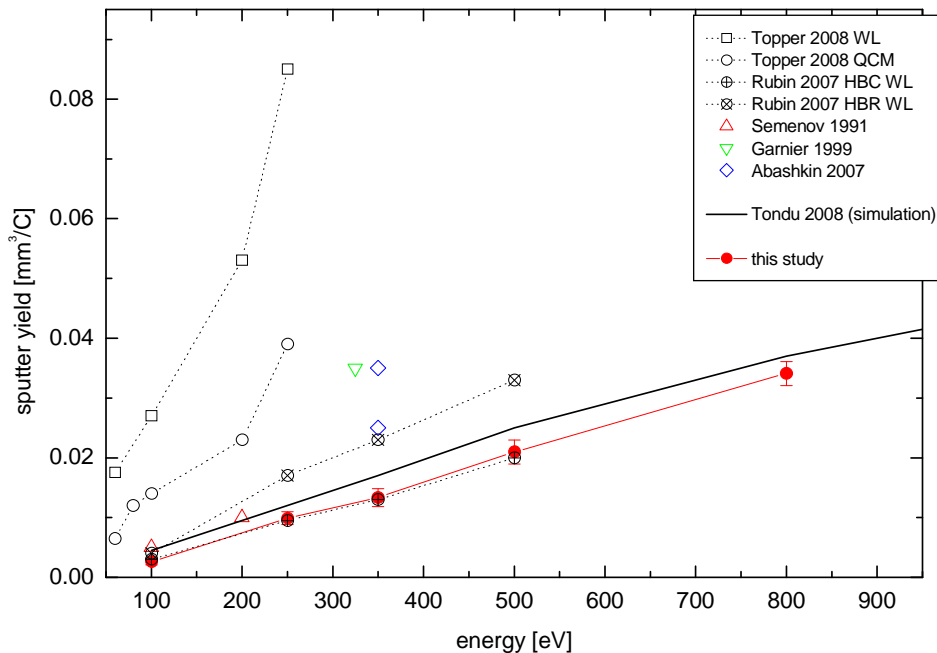


Figure 20: Sputter yield of BN in dependence on xenon ion energy (normal incidence).

V. Summary and Outlook

Measuring sputter yields of isolating materials is not a simple task. Many circumstances regarding the ion beam and target neutralization by electrons may affect the sputter result. The determination of the sputtering target current requires large attention.

The following table summarizes the measured sputter yields in mm³/C.

	Quartz	Al ₂ O ₃	BN
100 eV	0.0132	0.00189	0.00265
250 eV	0.0395	0.0076	0.01
350 eV	0.0577	0.013	0.0133
500 eV	0.076	0.0213	0.021
800 eV	0.118	0.0326	0.034

References

- ¹ M. Tartz, E. Hartmann, H. Neumann, *Validated simulation of the ion extraction grid lifetime*, Rev. Sci. Instrum. 79 (2008) 02B905; M. Tartz, E. Hartmann, H. Neumann, Paper Nr. AIAA-2006-5001, 42nd Joint Propulsion Conference, Sacramento, CA, 9.-12.7. 2006.
- ² S. Y. Cheng, M. Martinez-Sanchez, *Modeling of Hall thruster lifetime and erosion mechanisms*, IEPC-2007-250, 30th International Electric Propulsion Conference, Florence, Italy, 17. - 20.9. 2007.
- ³ M. Tartz, H. Neumann, *Sputter Yields of Carbon Materials under Xenon Ion Incidence*, Plasma Process. Polym. 4 (2007) S633.
- ⁴ M. Tartz, D. Manova, H. Neumann, H. Leiter, J. Esch, *Sputter investigation of ion thruster grid materials*, Paper Nr. AIAA-2005-4414, 41. Joint Propulsion Conference, Tucson, AZ, 10.-13.07. (2005)
- ⁵ M. Tartz, E. Hartmann, F. Scholze, H. Neumann, F. Bigl, *A new approach to ion beam modelling*, Surf. Coat. Technol. 97 (1997) 504.
- ⁶ F. Scholze, M. Tartz, H. Neumann, H. J. Leiter, R. Kukies, D. Feili, S. Weis, *Ion analytical characterisation of the RIT 22 ion thruster*, Paper Nr. AIAA-2007-5216, 43. Joint Propulsion Conference, Cincinnati, OH, 8.-11.7. (2007).
- ⁷ M. Zeuner, H. Neumann, F. Scholze, D. Flamm, M. Tartz, F. Bigl, *Characterization of a modular broad beam ion source*, Plasma Sources Sci. Technol. 7 (1998) 252-267.
- ⁸ R. Becker, W. B. Herrmannsfeldt, *“IGUN - A program for the simulation of positive ion extraction including magnetic fields”*, Rev. Sci. Instrum. 63 (1992) 2756-2758; R. Becker, *“New features in the simulation of ion extraction with IGUN”*, Proc. 6. Europ. Particle Accelerator Conf. EPAC98, 22.-26. Juni 1998, Stockholm.
- ⁹ R. L. Petry, Phys. Rev. 26 (1925) 346.
- ¹⁰ H. Bruining, J. H. de Boer, Physica V (1938) 2.
- ¹¹ A. Yalin, B. Rubin, S. Domingue, J. Williams, Z. Glueckert, *Differential Sputter Yields Of BN, Quartz, and Kapton By Xe+ Bombardment*, Paper AIAA-2007-5314, 43rd Joint Propulsion Conference, Cincinnati, OH, 9.-11.7.2007.
- ¹² Th. Tondou, V. Viel-Inguibert, J- F. Roussel, S. D'Escrivan, *Hall Effect Thrusters ceramics sputtering yield determination by Monte Carlo simulations*, Paper Nr. AIAA-2008-5090, 44th Joint Propulsion Conference, Hartford, CT, 21.-23.7. 2008.
- ¹³ B. Rubin, J. L. Topper, A. P. Yalin, *Total and Differential Sputter Yields Of Boron Nitride Measured by Quartz Crystal Microbalance and Weight Loss*, IEPC-2007-074, 30th International Electric Propulsion Conference, Florence, Italy, 17. - 20.9. 2007.
- ¹⁴ Semenov A., Shkarban, I., *Ion Beam Sputtering of the Surfaces of Ion and Plasma Sources*, Rocket and Space Engineering: Rocket Engines and Power Plants, No.3, 1991, 42.
- ¹⁵ Y. Garnier, V. Viel, J.-F. Roussel, J. Bernard, *Low-energy xenon ion sputtering of ceramics investigated for stationary plasma thrusters*, J. Vac. Sci. Tech. A 17 (6) pp. 3246-3254.
- ¹⁶ Abashkin, V., Gorshkov, O., Lovtsov, A., and Shagaida, A., *Analysis of Ceramic Erosion Characteristic in Hall-Effect Thruster with Higher Specific Impulse*, IEPC-2007-133, 30th International Electric Propulsion Conference, Florence, Italy, 17. - 20.9. 2007.
- ¹⁷ J. L. Topper, B. Rubin, C. C. Farnell, A. P. Yalin, *Preliminary Results of Low Energy Sputter Yields of Boron Nitride due to Xenon Ion Bombardment*, Paper AIAA-2008-5092, 44th Joint Propulsion Conference, Hartford, CT, 21.-23.7.2008.